This full text paper was peer reviewed at the direction of IEEE Communications Society subject matter experts for publication in the WCNC 2009 proceedings.

Pilot Designs for Channel Estimation of OFDM Systems with Frequency-Dependent I/Q Imbalances

Hlaing Minn and Daniel Munoz
Department of Electrical Engineering, University of Texas at Dallas, USA
Email: {hlaing.minn,daniel.munoz}@utdallas.edu

***Abstract*—The advances in semiconductor downscaling have empowered communication devices with significantly enhanced signal processing capability, but with the side effect of larger device impairments. Among those impairments, the I/Q imbalance is a critical one as it causes intercarrier interferences in orthogonal frequency division multiplexing (OFDM) systems. The I/Q imbalances in general exist at both transmitter and receiver, and they can be frequency-dependent. They may vary over time (e.g. due to sudden changes in temperature or the dynamics of the cooperating/relaying users). Under such scenarios, estimation and compensation of the combined effect of the channel and I/Q imbalances are crucial. This paper presents efficient pilot designs for such tasks. The advantages of the proposed designs over the existing ones in terms of estimation performance and overhead efficiency are corroborated by analysis and simulation results.**

***Index Terms*—Channel estimation, I/Q imbalance, OFDM, Pilot design**

I. INTRODUCTION

Most of the current and future wireless systems (e.g., IEEE 802.11a/g/n, 802.16a/e, LTE) have adopted orthogonal frequency division multiplexing/multiple-access (OFDM/OFDMA) which facilitates high data rate transmission in broadband channels with low complexity. Newer generation of wireless systems supports higher data rate by capitalizing on the increased signal processing capability fueled by semiconductor technology advances. The trend of successful semiconductor downscaling has resulted in smaller and cheaper devices with larger signal processing power but also with the side effect of exacerbation of device characteristics variations [1]. The gain and phase mismatch between the inphase and quadrature branches of a transceiver (known as I/Q imbalance) is a major one among such device impairments. Its effects are more prominent for direct conversion transceivers (typically used due to its cost-effectiveness) and higher modulation order (required for high data rate).

For OFDMA or wideband OFDM systems, I/Q imbalances can also be frequency-dependent, and exist at both transmitter and receiver, e.g., in mobile-to-mobile communications, or cooperative/relay communications. They can be time-variant as well (e.g., due to sudden temperature changes or dynamics of the cooperating or relaying users). Under these scenarios, it is much desirable to estimate the combined effect of the channel and I/Q imbalances for equalization and data detection. The efficient and practical approach for reliable estimation of the combined response is the use of pilot tones. This paper addresses pilot designs for such systems.

Recently, there have been several renewed interests in I/Q imbalance problems for OFDM systems in terms of estimation and compensation algorithms (e.g., [2]–[5]) and pilot designs (e.g., [6]–[12]). Existing pilot designs for OFDM channel estimation (e.g., [13]–[16]) do not take into account the I/Q imbalances and their performance can be significantly degraded in the presence of I/Q imbalances. On the other hand, the existing pilot designs for OFDM I/Q imbalance are associated with some of the following disadvantages – overhead-inefficiency, inapplicability for pilot-data-multiplexed setup, non-optimal estimation performance, no provision of channel estimates across the entire band, and unsuitability for OFDM systems with guard bands. Some of these designs consider receiver I/Q imbalance only or frequency-independent I/Q imbalance, while the others address both transmitter and receiver I/Q imbalances or/and frequency-dependent I/Q imbalances. A few of these designs address channel estimation separately, while most of them estimate the combined response of the channel and I/Q imbalance.

In this paper, we propose several pilot designs for estimating the combined response of the channel and I/Q imbalance in OFDM systems with both transmitter and receiver frequency-dependent I/Q imbalances. We derive pilot design conditions for optimal channel estimation as well as cancellation of I/Q imbalance introduced interferences, and develop several pilot designs satisfying these optimal conditions. Our designs overcome the disadvantages of the existing designs.

The rest of the paper is organized as follows. Section II describes signal model in the presence of frequency-independent and -dependent transmit and receive I/Q imbalances in OFDM systems. Section III presents pilot design criteria. In Section IV, we present our proposed pilot designs and their relationship to existing designs. Performance evaluation and simulation results are discussed in Section V, and conclusions are provided in Section VI.

II. SIGNAL MODEL

Let us consider a single antenna system with frequency-independent and frequency-dependent I/Q imbalances at both transmitter and receiver sides as shown in Fig. 1 where $\{a_t^I, a_t^Q\}$ and $\{\theta_t^I, \theta_t^Q\}$ represent frequency-independent gains and phase offsets of the I and Q branches at the transmitter. The equivalent pulse shaping filters (i.e., the overall impulse responses including DAC, amplifier, pulse shaping, and frequency-dependent imbalances) for the I and Q branches

978-1-4244-2948-6/09/$25.00 ©2009 IEEE

of the transmitter are denoted by $g_t^I(t)$ and $g_t^Q(t)$. The receiver side parameters are defined in the same manner with the subscript t replaced by r. An equivalent low-pass system is also presented in Fig. 1 where $h(t)$ is the low-pass-equivalent of the bandpass channel $h_{bp}(t)$. The transmit system with I/Q imbalance can be viewed as the summation of two systems namely direct system whose input is the same as the transmitter input signal $s(t) = s_I(t) + js_Q(t)$ and mirror system whose input is $s^*(t)$. The impulse responses of the direct and mirror systems at the transmitter are denoted by $g_T^D(t)$ and $g_T^M(t)$, and those at the receiver are represented by $g_R^D(t)$ and $g_R^M(t)$, respectively. They are related to the I/Q imbalance parameters and the equivalent pulse shaping filters as

$$g_T^D(t) = \frac{1}{2}[a_t^I e^{j\theta_t^I} g_t^I(t) + a_t^Q e^{j\theta_t^Q} g_t^Q(t)] \quad (1)$$

$$g_T^M(t) = \frac{1}{2}[a_t^I e^{j\theta_t^I} g_t^I(t) - a_t^Q e^{j\theta_t^Q} g_t^Q(t)] \quad (2)$$

$$g_R^D(t) = \frac{1}{2}[a_r^I e^{-j\theta_r^I} g_r^I(t) + a_r^Q e^{-j\theta_r^Q} g_r^Q(t)] \quad (3)$$

$$g_R^M(t) = \frac{1}{2}[a_r^I e^{j\theta_r^I} g_r^I(t) - a_r^Q e^{j\theta_r^Q} g_r^Q(t)]. \quad (4)$$

The equivalent direct channel and mirror channel (including the transmit and receive filters as well as the channel $h(t)$) are given as

$$p(t) = g_T^D(t) * h(t) * g_R^D(t) + (g_T^M(t))^* * h^*(t) * g_R^M(t) \quad (5)$$

$$q(t) = g_T^M(t) * h(t) * g_R^D(t) + (g_T^D(t))^* * h^*(t) * g_R^M(t). \quad (6)$$

Finally, the received signal can be written as

$$r(t) = s(t) * p(t) + s^*(t) * q(t) + n(t) \quad (7)$$

where the complex Gaussian noise $n(t)$ is given by

$$n(t) = w(t) * g_R^D(t) + w^*(t) * g_R^M(t). \quad (8)$$

We consider an OFDM system with a cyclic prefix (CP) interval (N_{CP} samples) longer than the maximum span (L samples) of $p(t)$ and $q(t)$.

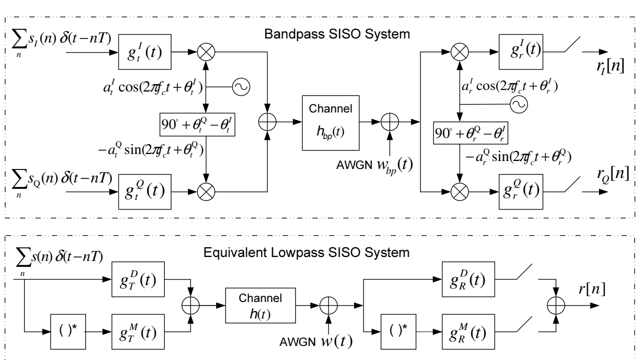

Fig. 1. Bandpass and equivalent lowpass SISO system models with frequency-independent and frequency-dependent I/Q imbalances

Now, let us consider a low-pass-equivalent discrete-time OFDM system with N subcarriers. The channels are assumed to be constant over Q symbol intervals. The discrete-time transmit training signal during the lth symbol duration is denoted by $s^{(l)}[k]$ with the integer index $k \in [-N_{\mathrm{CP}}, N-1]$, and the CP samples $s^{(l)}[-m] = s^{(l)}[N-m]$ for $m \in [-N_{\mathrm{CP}}, -1]$. Similar notations apply to data signal $x^{(l)}[k]$. The discrete-time versions of $p(t)$ and $q(t)$ are denoted by $L \times 1$ vectors $\boldsymbol{p}$ and $\boldsymbol{q}$, respectively. The $N \times 1$ received signal vector after CP removal for the lth OFDM symbol is denoted by $\boldsymbol{r}_l$. In a general pilot-data multiplexed setup (which includes pilot only or data only symbols as special cases), the received vector $\boldsymbol{r}_l$ can be expressed in a matrix form as

$$\boldsymbol{r}_l = (\boldsymbol{S}[l] + \boldsymbol{X}[l])\boldsymbol{p} + (\boldsymbol{S}^*[l] + \boldsymbol{X}^*[l])\boldsymbol{q} + \boldsymbol{n}_l \quad (9)$$

where (m, k)th element of the $N \times L$ signal matrix $\boldsymbol{S}[l]$ (or $\boldsymbol{X}[l]$) is $s^{(l)}[m-k]$ (or $x^{(l)}[m-k]$) with $m \in [0, N-1]$ and $k \in [0, L-1]$.

In a more compact form, the time-domain received signal vector after CP removal for Q OFDM symbols is given by

$$\boldsymbol{r} = \boldsymbol{S}\boldsymbol{p} + \boldsymbol{S}^*\boldsymbol{q} + \boldsymbol{X}\boldsymbol{p} + \boldsymbol{X}^*\boldsymbol{q} + \boldsymbol{n} \quad (10)$$

where

$$\boldsymbol{r} = [\boldsymbol{r}_0^T \boldsymbol{r}_1^T \ldots \boldsymbol{r}_{Q-1}^T]^T \quad (11)$$

$$\boldsymbol{n} = [\boldsymbol{n}_0^T \boldsymbol{n}_1^T \ldots \boldsymbol{n}_{Q-1}^T]^T \quad (12)$$

$$\boldsymbol{S} = \left[\boldsymbol{S}_0^T[0], \boldsymbol{S}_0^T[1], \ldots, \boldsymbol{S}_0^T[Q-1]\right]^T, \quad (13)$$

$$\boldsymbol{X} = \left[\boldsymbol{X}_0^T[0], \boldsymbol{X}_0^T[1], \ldots, \boldsymbol{X}_0^T[Q-1]\right]^T. \quad (14)$$

The complex Gaussian noise vectors $\{\boldsymbol{n}_l\}$ are given by

$$\boldsymbol{n}_l = \boldsymbol{G}_{R,D}\boldsymbol{w}_l + \boldsymbol{G}_{R,Q}\boldsymbol{w}_l^* \quad (15)$$

where $\{\boldsymbol{w}_l\}$ are independent and identically distributed (iid) random vectors consisting of iid circularly-symmetric complex Gaussian random variables with the variance σ_w^2. Let λ denote the maximum of the number of taps of $g_R^D[k]$ and $g_R^Q[k]$. Then, $\boldsymbol{G}_{R,D}$ and $\boldsymbol{G}_{R,Q}$ are $N \times (N + \lambda)$ matrices with their first rows given by $[g_R^D[0], g_R^D[1], \ldots, g_R^D[\lambda], \boldsymbol{0}_{N-1}]$ and $[g_R^Q[0], g_R^Q[1], \ldots, g_R^Q[\lambda], \boldsymbol{0}_{N-1}]$, respectively, and their next kth rows are k-cyclic-shift (clockwise) versions of their corresponding first rows.

III. OFDM Pilot Design Criteria

For coherent detection, the direct channel $\boldsymbol{p}$ and the mirror channel $\boldsymbol{q}$ need to be estimated at the receiver. In practical systems, the statistics of the channel and the transceiver imperfections are unknown and they can be non-stationary as well. This leads to the practical choice of least-squares type channel estimators as considered in this paper. The estimates of the direct and mirror CIR vectors are given by

$$\hat{p} = \left(\boldsymbol{S}^H\boldsymbol{S}\right)^{-1}\boldsymbol{S}^H\boldsymbol{r} \quad (16)$$

$$\hat{q} = \left(\boldsymbol{S}^T\boldsymbol{S}^*\right)^{-1}\boldsymbol{S}^T\boldsymbol{r}. \quad (17)$$

Our pilot designs will be based on minimizing the mean-square error (MSE) of the channel estimation.

Substituting (10) into (16) and (17) gives

$$\hat{\boldsymbol{p}} = \left(\boldsymbol{S}^H\boldsymbol{S}\right)^{-1}\boldsymbol{S}^H\boldsymbol{S}\boldsymbol{p} + \left(\boldsymbol{S}^H\boldsymbol{S}\right)^{-1}\boldsymbol{S}^H\boldsymbol{S}^*\boldsymbol{q} + \left(\boldsymbol{S}^H\boldsymbol{S}\right)^{-1}\boldsymbol{S}^H\boldsymbol{X}\boldsymbol{p} + \left(\boldsymbol{S}^H\boldsymbol{S}\right)^{-1}\boldsymbol{S}^H\boldsymbol{X}^*\boldsymbol{q} + \left(\boldsymbol{S}^H\boldsymbol{S}\right)^{-1}\boldsymbol{S}^H\boldsymbol{n} \quad (18)$$

$$\hat{\boldsymbol{q}} = \left(\boldsymbol{S}^T\boldsymbol{S}^*\right)^{-1}\boldsymbol{S}^T\boldsymbol{S}\boldsymbol{p} + \left(\boldsymbol{S}^T\boldsymbol{S}^*\right)^{-1}\boldsymbol{S}^T\boldsymbol{S}^*\boldsymbol{q} + \left(\boldsymbol{S}^T\boldsymbol{S}^*\right)^{-1}\boldsymbol{S}^T\boldsymbol{X}\boldsymbol{p} + \left(\boldsymbol{S}^T\boldsymbol{S}^*\right)^{-1}\boldsymbol{S}^T\boldsymbol{X}^*\boldsymbol{q} + \left(\boldsymbol{S}^T\boldsymbol{S}^*\right)^{-1}\boldsymbol{S}^T\boldsymbol{n}. \quad (19)$$

We observe the following conditions for the pilot designs:

1) Estimation Identifiability Condition: The identifiability of $\boldsymbol{p}$ and $\boldsymbol{q}$ estimation requires that $\boldsymbol{S}^H\boldsymbol{S}$ is of full-rank.
2) Zero Cross Channel Interference Condition: The MSE due to the second term (cross channel interference) in (18) and (19) is minimized (completely removed) when $\boldsymbol{S}^H\boldsymbol{S}^*$ equals to the $L \times L$ all zero matrix $\mathbf{0}_L$.
3) Zero Data Interference Condition: The random data interference is completely suppressed when $\boldsymbol{S}^H\boldsymbol{X} = \mathbf{0}_L$ and $\boldsymbol{S}^H\boldsymbol{X}^* = \mathbf{0}_L$.
4) White Noise Optimality Condition: When the equivalent receive-filter is a square-root Nyquist filter, the MSE due to the noise is minimized when $\boldsymbol{S}^H\boldsymbol{S} = E_Q\boldsymbol{I}_L$ where E_Q is the total energy of the transmit pilot signal vector over Q symbols (excluding CPs), and $\boldsymbol{I}_L$ is the $L \times L$ identity matrix. The frequency-flat receiver I/Q imbalance with a square-root raised cosine receive filter represents this scenario.
5) For the scenario with frequency-selective receiver I/Q imbalance, the noise covariance matrix is unknown a priori, and hence it is infeasible to develop optimal pilot designs. However, frequency selectivity of the receiver I/Q imbalance is typically very small. A practical approach in this case is to assume frequency-flat receiver I/Q imbalance in the pilot designs which leads to the requirement of $\boldsymbol{S}^H\boldsymbol{S} = E_Q\boldsymbol{I}_L$.

When the identifiability condition and the zero data interference condition are satisfied, the MSEs of $\boldsymbol{p}$ and $\boldsymbol{q}$ estimation are given by

$$\mathrm{MSE}_{\boldsymbol{p}} = \mathrm{Tr}\left[\left(\boldsymbol{S}^H\boldsymbol{S}\right)^{-1}\boldsymbol{S}^H\boldsymbol{S}^*E[\boldsymbol{q}\boldsymbol{q}^H]\boldsymbol{S}^T\boldsymbol{S}\left(\boldsymbol{S}^H\boldsymbol{S}\right)^{-1} + \left(\boldsymbol{S}^H\boldsymbol{S}\right)^{-1}\boldsymbol{S}^H\boldsymbol{C}_{\boldsymbol{n}}\boldsymbol{S}\left(\boldsymbol{S}^H\boldsymbol{S}\right)^{-1}\right] \quad (20)$$

$$\mathrm{MSE}_{\boldsymbol{q}} = \mathrm{Tr}\left[\left(\boldsymbol{S}^T\boldsymbol{S}^*\right)^{-1}\boldsymbol{S}^T\boldsymbol{S}E[\boldsymbol{p}\boldsymbol{p}^H]\boldsymbol{S}^H\boldsymbol{S}^*\left(\boldsymbol{S}^T\boldsymbol{S}^*\right)^{-1} + \left(\boldsymbol{S}^T\boldsymbol{S}^*\right)^{-1}\boldsymbol{S}^T\boldsymbol{C}_{\boldsymbol{n}}\boldsymbol{S}^*\left(\boldsymbol{S}^T\boldsymbol{S}^*\right)^{-1}\right] \quad (21)$$

where the noise covariance matrix $\boldsymbol{C}_{\boldsymbol{n}}$ is given by

$$\boldsymbol{C}_{\boldsymbol{n}} = \sigma_w^2(\boldsymbol{G}_{R,D}\boldsymbol{G}_{R,D}^H + \boldsymbol{G}_{R,Q}\boldsymbol{G}_{R,Q}^H) \otimes \boldsymbol{I}_Q \quad (22)$$

and $\otimes$ denotes the Kronecker product.

If the zero cross channel interference condition is also met, the above MSE expressions become

$$\mathrm{MSE}_{\boldsymbol{p}} = \mathrm{Tr}\left[\left(\boldsymbol{S}^H\boldsymbol{S}\right)^{-1}\boldsymbol{S}^H\boldsymbol{C}_{\boldsymbol{n}}\boldsymbol{S}\left(\boldsymbol{S}^H\boldsymbol{S}\right)^{-1}\right] \quad (23)$$

$$\mathrm{MSE}_{\boldsymbol{q}} = \mathrm{Tr}\left[\left(\boldsymbol{S}^T\boldsymbol{S}^*\right)^{-1}\boldsymbol{S}^T\boldsymbol{C}_{\boldsymbol{n}}\boldsymbol{S}^*\left(\boldsymbol{S}^T\boldsymbol{S}^*\right)^{-1}\right]. \quad (24)$$

Additionally, if demodulator output noise samples are white (i.e., $\boldsymbol{C}_{\boldsymbol{n}} = \sigma_w^2\boldsymbol{I}_{NQ}$), the MSE expressions simplify to

$$\mathrm{MSE}_{\boldsymbol{p}} = \mathrm{MSE}_{\boldsymbol{q}} = \sigma_n^2\mathrm{Tr}\left[\left(\boldsymbol{S}^H\boldsymbol{S}\right)^{-1}\right]. \quad (25)$$

In summary, the OFDM pilot design criterion satisfying estimation identifiability, zero data interference condition, zero cross channel interference, and white noise optimality reads as

$$\left.\begin{array}{l}\left(\boldsymbol{S}^H\boldsymbol{S}\right) = E_Q\boldsymbol{I}_L \;\;\&\;\; \left(\boldsymbol{S}^H\boldsymbol{S}^*\right) = \mathbf{0}_L \\ \boldsymbol{S}^H\boldsymbol{X} = \mathbf{0}_L \;\;\&\;\; \boldsymbol{S}^H\boldsymbol{X}^* = \mathbf{0}_L\end{array}\right\} \quad (26)$$

which serves as our pilot design criterion.

Let $c_l[k]$ denote the pilot symbol on the kth subcarrier of the lth OFDM symbol. Define $\mathcal{J}_l$ and $\mathcal{I}_l$ as the pilot (including null pilot) tone index set and the data tone index set during the lth OFDM symbol, respectively. The tone indexes of a mirror pair is given by $(k, -k)$ for $k = 0, 1, \ldots, N/2$ where a modulo-N is implicitly assumed for the tone indexes. Note that $k = 0$ is a self-mirror tone and so is $k = N/2$. We assume the FFT size N is a power of two, as typically used in practice. Also define $L_0 = 2^{\lceil \log_2(L) \rceil}$, $L_i = 2^i L_0$ and $M_i = N/L_i$.

From the above pilot design criteria, we obtain the following conditions[1] on the pilot and data tones. The zero data-interference condition is met by choosing the pilot tone indexes to be from mirror pairs. The estimation identifiability and MSE optimality conditions are satisfied if

$$\sum_{k=0}^{N-1}\left(\sum_{l=0}^{Q-1}|c_l[k]|^2\right)e^{j2\pi dk/N} = E_Q\delta[d], \quad (27)$$
$$\text{for} \quad d \in \{-L+1, -L+2, \ldots, L-1\}.$$

The zero mirror pilot interference condition is met when

$$\sum_{k=0}^{N-1}\left(\sum_{l=0}^{Q-1}c_l[k]c_l[N-k]\right)e^{j2\pi dk/N} = 0, \quad (28)$$
$$\text{for } d \in \{-L+1, -L+2, \ldots, L-1\}.$$

IV. OFDM Pilot Designs

We present our pilot designs without detailed derivations as they can be straightly proved to satisfy our design conditions. Examples of our pilot designs are provided in Tables I and II for illustration of the concepts where parameters are chosen for the convenience of the presentation.

A. Designs Using One Symbol

We present two designs using one pilot-data multiplexed symbol (i.e., $Q = 1$), and the symbol index l is omitted.

[1]Due to the space limitation, we omit details of how they are derived.

1) Frequency-Domain Coding (FDC): In this design, the pilot and data index sets are given by

$$\mathcal{J} = \{0, M_0/2, M_0, \ldots, N - M_0/2\} \quad (29)$$

$$\mathcal{I} = \{0, 1, 2, \ldots, N-1\} \setminus \mathcal{J}. \quad (30)$$

The mirror tone interferences are suppressed by FDC as follows. The pilots at $k = 0$ and $k = N/2$ are given by

$$c[0] = \pm c[N/2] = \pm 1 \text{ or } \pm j. \quad (31)$$

For pilots at $k < N/2$, the values can be unit amplitude with arbitrary phase ϕ_k. For $k > N/2$, they are alternating positive and negative unit amplitudes with the same phase as their corresponding mirror tone. The pilots can be assigned as:

$$c[k] = e^{j\phi_k}, \text{ arbitrary } \phi_k, \; k \in \mathcal{J} \;\&\; 0 < k < \frac{N}{2} \quad (32)$$

$$c[k] = (-1)^{\frac{2k-N}{M_0}} c^2[0] c^*[-k], \; k \in \mathcal{J} \;\&\; \frac{N}{2} < k < N \quad (33)$$

$$c[k] = 0, \; k \notin \mathcal{J}. \quad (34)$$

The above pilot codes across the frequency domain are designed such that the mirror interference becomes zero, i.e., to satisfy (28). It should be noted that this design requires the use of $k = 0$ and $k = N/2$ for optimum MSE performance, so if a guard band is necessary at these tones, this design will experience some interference.

2) Frequency-Domain Nulling (FDN): This design suppresses mirror tone interferences by means of mirror null tones while having non-zero pilot tones with equal spacing (cyclically) for estimation optimality. It consists of L_n ($\leq N/2$) constant amplitude pilot tones with the index set $\mathcal{J}^{\text{pilot}}$ and L_n null tones with the index set $\mathcal{J}^{\text{null}}$. Define $\mathcal{T}_{n,k} \triangleq [k, k+M_n, k+2M_n, \ldots, k+N-M_n]$ which consists of cyclically equi-spaced L_n indexes from $[0, N-1]$, and $k \in \{\{1, 2, \ldots, M_n - 1\} \setminus \{M_n/2\}\}$. Then the index sets are given by

$$\mathcal{J}^{\text{pilot}} = \mathcal{T}_{n,k}, \; k \in \{\{1, 2, \ldots, M_n - 1\} \setminus \{M_n/2\}\} \quad (35)$$

$$\mathcal{J}^{\text{null}} = \{N - \mathcal{J}^{\text{pilot}}\} \quad (36)$$

$$\mathcal{J} = \{\mathcal{J}^{\text{pilot}} \cup \mathcal{J}^{\text{null}}\} \quad (37)$$

$$\mathcal{I} = \{0, 1, \ldots, N-1\} \setminus \mathcal{J}. \quad (38)$$

The pilot tones are given by

$$\boldsymbol{c}[k] = e^{j\phi_k}, \text{ arbitrary } \phi_{\text{k}}, \; k \in \mathcal{J}^{\text{pilot}} \quad (39)$$

$$\boldsymbol{c}[k] = 0, \; k \notin \mathcal{J}^{\text{pilot}}. \quad (40)$$

The choice of M_0 for M_n gives the best overhead efficiency.

B. Designs Using Multiple Symbols

An advantage of using multiple symbols over one symbol for pilot design is a better flexibility in accommodating null guard bands for practical systems. In the design using one symbol, cyclically-equal spacing of non-zero pilot tones is required for the estimation optimality while additional set of equal-spacing pilot tone set (either null or non-zero) is used for mirror tone interference cancellation. These pilot tone locations and spacings determine the amount of allowable null guard band. To accommodate a larger guardband, a larger pilot tone spacing would be necessary, while a larger channel length will require a smaller pilot tone spacing. This conflicting constraint can be alleviated by the use of multiple pilot symbols, where we can have less pilots in use in each symbol so a larger spacing between pilot tones can be achieved. Another advantage of using multiple pilot symbols is its flexibility in satisfying the zero mirror tone interference condition such that the mirror tone interference need not be zero within each symbol, but rather the sum of the mirror tone interferences over the multiple symbols is required to be zero.

1) Time and Frequency Domain Coding (TFDC): For overhead efficiency, we adopt the pilot and data index sets as

$$\mathcal{J}_l = \{M_0/2, 3M_0/2, 5M_0/2, \ldots, N - M_0/2\}, \quad (41)$$

$$\mathcal{I}_l = \{0, 1, 2, \ldots, N-1\} \setminus \mathcal{J}_l \quad (42)$$

although M_i can be used in place of M_0. The above index sets also provide greater flexibility for guardband insertion than the design using one symbol. The choice of $Q = 2$ requires minimum overhead, but in the following we will describe our pilot designs using $Q \geq 2$ pilot-data-multiplexed symbols. The total energy over Q symbols of the pilot on the kth tone is the same for $k \in \mathcal{J}_l$. A general design is defined as follows. For $k \in \mathcal{J}_l$ and $k < N/2$,

$$c_l[k] = e^{j\phi_{l,k}}, \text{ arbitrary } \{\phi_{l,k}\}, \quad (43)$$

$$c_0[-k] = e^{j\theta}, \text{ arbitrary } \theta, \quad (44)$$

$$c_l[-k] = e^{j2\pi\tau l/Q} c_0[k] c_0[-k] / c_l[k], \quad (45)$$

$$\tau \in \{1, 2, \ldots, Q-1\}, \; l = 1, \ldots, Q-1.$$

If we set $c_0[k] = c_0[-k]$, $c_1[k] = c_0[k]$, and $Q = 2$ (hence $\tau = 1$), then $c_1[-k] = -c_0[k]$, and this design becomes that in [7], [8], [10] with an optimized pilot index set. If $c_1[k] = jc_0[k]$ with $Q = 2$, then $c_1[-k] = jc_0[-k]$, and this design becomes one of the two designs in [10] with an optimized pilot index set. Note that these existing designs did not consider estimation MSE optimality and overhead minimization, i.e., their pilot index sets are not optimized.

2) Reciprocal Frequency Domain Nulling (RFDN): This design also adopts the same pilot and data index sets of TFDC design for the same reasons of overhead efficiency and flexibility in guardband insertion. The difference from TFDC design is that this design uses null tones (hence $\mathcal{J}_l$ represents indexes of non-zero as well as null pilot tones) to avoid mirror tone interferences. Since the total pilot energy over Q symbols of the kth tone needs to be the same for all $k \in \mathcal{J}_l$, the nulling has to be reciprocal. In other words, if pilot on tone k is non-zero and on tone $-k$ is zero for the lth symbol, then there should be another symbol where pilot on tone k is zero and on tone $-k$ is nonzero. With this reciprocal nulling, the minimum value of Q is 2, and the maximum is L_0. When $Q = 2$, $\mathcal{J}_l$ is divided into two subset of size $L_0/2$ such that the indexes in one subset are exactly the mirror indexes of those in the other subset. In the first symbol, non-zero constant amplitude

TABLE I
EXAMPLES OF PILOT DESIGNS USING ONE SYMBOL WHERE $\{a_k\}$ ARE UNIT-AMPLITUDE ARBITRARY SYMBOLS AND $N = 64$

Design	symbol index l	Pilots
FDC $Q = 1$, $L_0 = 4$, $M_0 = 16$	0	$\mathcal{J} = \{0, 8, 16, 24, 32, 40, 48, 56\}$ $c[k \in \mathcal{J}] = \{j, a_1, a_2, a_3,$ $j, a_3^*, -a_2^*, a_1^*\}$
FDN $Q = 1$, $L_0 = 4$, $M_0 = 16$	0	$\mathcal{J}^{\text{pilot}} = \{1, 17, 33, 49\}$ $\mathcal{J}^{\text{null}} = \{15, 31, 47, 63\}$ $c[k \in \mathcal{J}^{\text{pilot}}] = \{a_1, a_2, a_3, a_4\}$

TABLE II
EXAMPLES OF PILOT DESIGNS USING MULTIPLE SYMBOLS WHERE $\{a_k\}$ ARE CONSTANT-AMPLITUDE ARBITRARY SYMBOLS AND $N = 64$

Design	symbol index l	Pilots
TFDC		$\mathcal{J} = \{8, 24, 40, 56\}$
	0	$c_0[k \in \mathcal{J}] = \{a_1, a_2, a_3, a_4\}$
$Q = 4$, $L_0 = 4$,	1	$c_1[k \in \mathcal{J}] = \{a_1, a_2, ja_3, ja_4\}$
$M_0 = 16$	2	$c_2[k \in \mathcal{J}] = \{a_1, a_2, -a_3, -a_4\}$
	3	$c_3[k \in \mathcal{J}] = \{a_1, a_2, -ja_3, -ja_4\}$
RFDN		$\mathcal{J} = \{8, 24, 40, 56\}$
$Q = 2$, $L_0 = 4$,	0	$c_0[k \in \mathcal{J}] = \{a_1, 0, a_2, 0\}$
$M_0 = 16$	1	$c_0[k \in \mathcal{J}] = \{0, a_3, 0, a_4\}$

arbitrary pilot symbols are transmitted on one of the subsets and null pilots on the other subset. In the second symbol, the positions of non-zero arbitrary pilots and null pilots are switched. If the two subset of $\mathcal{J}_l$ are chosen such that one contains those less than $N/2$, then this design becomes that in [6], [9] with an optimized pilot index set.

V. SIMULATION RESULTS AND DISCUSSIONS

System parameters in the simulation are $N = 64$, 5 null guard tones at the band edges, M-ary QAM with $M = 4, 16, 64$, and a Rayleigh fading channel with $L = 8$. The frequency-independent I/Q imbalances are set to $\alpha = \frac{a_t^I}{a_t^Q} = \frac{a_r^I}{a_r^Q} = 0.4$ dB, and $\Delta\theta = \theta_t^I - \theta_t^Q = \theta_r^I - \theta_r^Q = 4°$. The frequency-dependent I/Q imbalances are modelled by 3-tap filters with discrete-time impulse responses of $[0.01, 0.9999, 0.01]$ and $[0.015, 0.9998, 0.01]$ for the transmit I and Q branches, and $[0.012, 0.9997, 0.018]$, and $[0.01, 0.9997, 0.02]$ for the receive I and Q branches. All of the proposed pilot designs give the same estimation performance and hence we use FDN design only. As a reference, we evaluate the design proposed in [12] with null guard tones according to the above setting. In all methods, the maximum likelihood detection is applied. In the reference method, the energy of each non-zero pilot tone is kept the same as that of data tone. For a fair comparison, total pilot energies of the two methods are set the same.

Figs. 2 and 3 present data MSE for 16-QAM and 64-QAM (MSE between received data and reconstructed received data based on correct data and estimated channels) as a measure of the channel estimation performance of different pilot designs. Due to the null guard tones, the reference design loses estimation optimality and experiences an MSE floor. The proposed design does not give an MSE floor and substantially outperforms the reference design.

In Figs. 4, 5, and 6, the (uncoded) BER performances of different pilot designs are compared. Similar conclusions for the MSE performance apply for the BER performance as well.

Table III compares pilot overhead of the proposed designs and the reference design. The proposed designs require only $2L_0$ tones if using one symbol, and QL_0 tones if utilizing more than one symbol as opposed to N tones of the reference design. In addition, the proposed designs can be applied in pilot-data multiplexed symbols as well as systems with guard null tones where the reference design does not fit well.

TABLE III
PILOT OVERHEAD COMPARISON

Design	Overhead (# of Tones)
FDC	$2L_0$
FDN	$2L_0$
TFDC	QL_0
RFDN	QL_0
Design from [12]	N

VI. CONCLUSIONS

We have presented efficient pilot designs for estimating the combined effects of the multipath channel and the frequency-dependent transmit and receive I/Q imbalances in OFDM systems. We decompose such a system into the direct channel and the mirror channel, and develop pilot designs for estimation of their impulse responses. The design criteria include zero cross channel interference between the direct and mirror channels and zero interference between pilot and data, in addition to the estimation identifiability and estimation MSE optimality conditions of the existing pilot designs for OFDM without I/Q imbalance. Our pilot designs provide better estimation and overhead efficiency than the existing pilot designs for OFDM with or without I/Q imbalance. Further investigation for MIMO OFDM systems with frequency-dependent transmit and receive I/Q imbalances is underway.

REFERENCES

[1] B. Razavi, "RF Microelectronics," *Prentice-Hall*, NJ, 1998.

[2] M. Valkama, M. Renfors, and V. Koivunen, "Compensation of frequency-selective I/Q imbalances in wideband receivers: models and algorithms," *IEEE SPAWC,* Mar. 2001, pp. 42–45.

[3] J. Tubbax, B. Come, L. Van der Perre, S. Donnay, M. Engels, M. Moonen, and H. De Man, "Joint compensation of IQ imbalance and frequency offset in OFDM systems," RAWCON, 2003, pp. 39–42.

[4] A. Tarighat and A. H. Sayed, "Joint compensation of transmitter and receiver impairments in OFDM systems," *IEEE Trans. Wireless Commun.,* vol. 6, no. 1, pp. 240–247, Jan. 2007.

[5] D. Tandur and M. Moonen, "Joint adaptive compensation of transmitter and receiver IQ imbalance under carrier frequency offset in OFDM-based systems," *IEEE Trans. Signal Process.,* 2007, vol. 5, pp. 5246–5252.

[6] W. Kirkland and K. Teo, "I/Q distortion correction for OFDM direct conversion receiver," *Electronics Letters*, 2003, vol. 39, pp. 131-133.

[7] L. Brotje, S. Vogeler, K-D. Kammeyer, "Estimation and correction of transmitter-caused I/Q imbalance in OFDM systems, *Proc. 7th Intl. OFDM Workshop,* Sept. 2002, pp. 178–182.

[8] Y. Egashira, Y. Tanabe, and K. Sato, "A novel IQ imbalance compensation method with pilot-signals for OFDM system," *IEEE VTC Fall*, 2006, pp. 1–5.

[9] A. Tarighat, R. Bagheri, and A. Sayed, "Compensation schemes and performance analysis of IQ imbalances in OFDM receivers," *IEEE Trans. Signal Process.,* 2005, vol. 53, pp. 3257–3268.

[10] R. Chrabieh and S. Soliman, "IQ imbalance mitigation via unbiased training sequences," *Proc. IEEE GLOBECOM,* 2007, pp. 4280–4285.

[11] E. Lopez-Estraviz, S. De Rore, F. Horlin, and L. Van der Perre, "Optimal training sequences for joint channel and frequency-dependent IQ imbalance estimation in OFDM-based receivers," *IEEE ICC* 2006, vol. 10, pp. 4595-4600.

[12] E. Lopez-Estraviz, S. De Rore, F. Horlin, and A. Bourdoux, "Pilot design for joint channel and frequency-dependent transmit/receive IQ imbalance estimation and compensation in OFDM-based transceivers," *IEEE ICC* 2007, pp. 4861-4866.

[13] I. Barhumi, G. Leus, and M. Moonen, "Optimal training design for MIMO OFDM systems in mobile wireless channels," *IEEE Trans. Signal Process.*, vol. 51, no. 6, pp. 1615–1624, Jun. 2003.

[14] H. Minn and N. Al-Dhahir, "Optimal training signals for MIMO OFDM channel estimation," *IEEE Trans. Wireless Commun.*, vol. 5, no. 5, pp. 1158–1168, May 2006.

[15] H. Minn, N. Al-Dhahir, Y. Li, "Optimal training signals for MIMO OFDM channel estimation in the presence of frequency offset and phase noise," *IEEE Trans. Commun.*, vol. 54, pp. 1754–1759, Oct. 2006.

[16] X. Ma, L. Yang, and G. B. Giannakis, "Optimal training for MIMO frequency-selective fading channels," *IEEE Trans. Wireless Commun.*, vol. 4, no. 2, pp. 453–466, Mar. 2005.

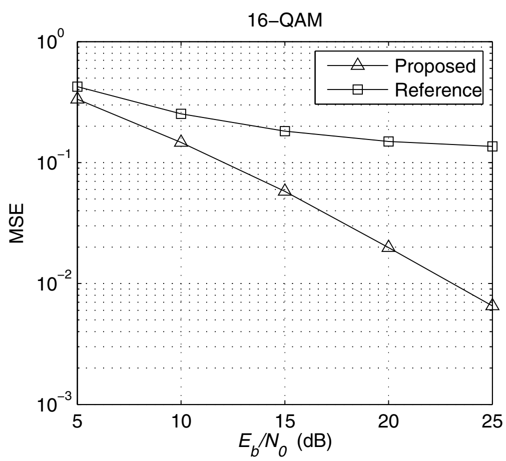

Fig. 2. Data MSE comparison of different pilot designs for 16-QAM

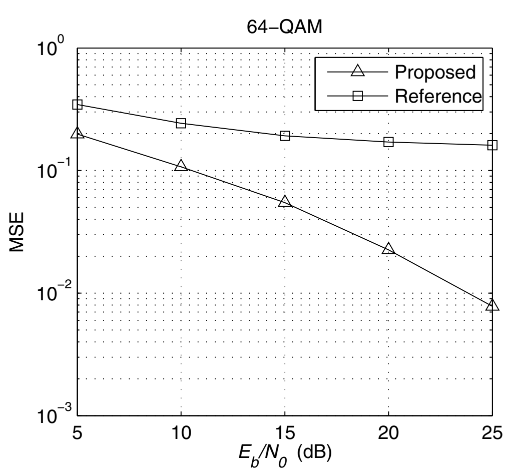

Fig. 3. Data MSE comparison of different pilot designs for 64-QAM

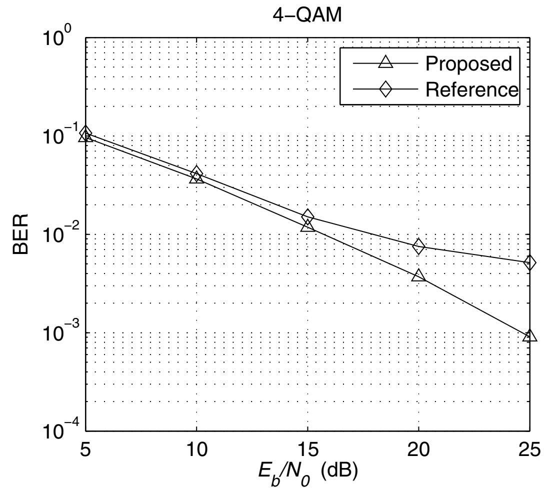

Fig. 4. BER comparison of different pilot designs for 4-QAM

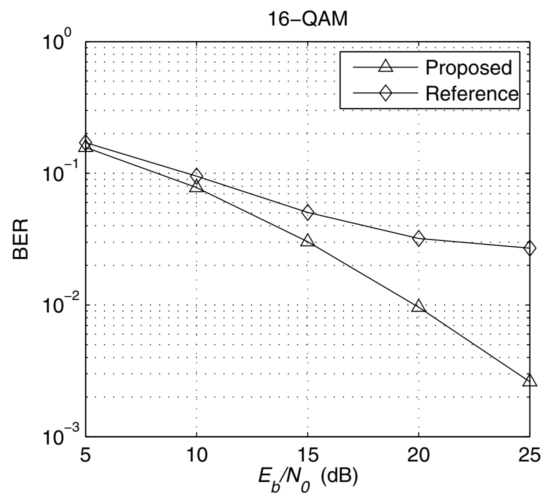

Fig. 5. BER comparison of different pilot designs for 16-QAM

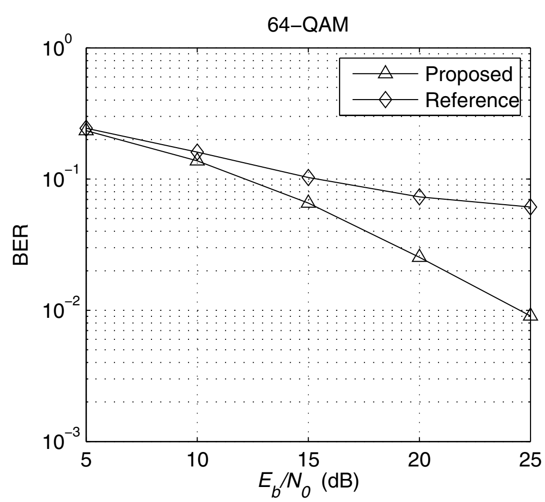

Fig. 6. BER comparison of different pilot designs for 64-QAM